

POLYESTER FABRICS COVERED WITH ZNO PARTICLES: PARTICLE INTERACTION WITH THE SURFACE SHOWN BY DIELECTRIC PROPERTIES

C. P. GANEA, L. FRUNZA*, I. ZGURA, N. PREDA, E. MATEI, S. FRUNZA
National institute of Materials Physics, 077125 Magurele, Romania

Polyester fabrics modified with ZnO particles by electroless deposition were investigated by broadband dielectric spectroscopy in a parallel capacitor between 10^{-2} and 10^7 Hz in a temperature interval from ca. 123 to 473 K. Textile samples were routinely characterized for the structure and interaction of the ZnO particles with the fiber surface. Since a textile fabric material is a mixture of air and fibers, the parameters taken into consideration should be called as effective ones. The deposition of ZnO particles lead to complex dielectric spectra and to the temperature dependence of the decomposed peaks following Arrhenius law.

(Received October 6, 2014; Accepted November 20, 2014)

Keywords: Dielectric loss, Permittivity, Textile fibers, Fabrics, Woven composites

1. Introduction

It is well known that textile materials are mostly dielectrics. Thus, dielectric properties and the electrical resistance give the static electricity during the textile contact with other objects, having a negative influence upon their behavior both in the use and processing. This is why these properties have been studied for a long time and are still much investigated in connection with the appearance of new synthetic textiles and of textile functionalization despite the difficulties related to the measurements of dielectric permittivity for (even flat) textiles and to find their relaxation mechanisms [1]. For example, cellulose was extensively investigated from this point of view starting from mid of 20th century (as mentioned in Bal and Kothari's review [2]) and arriving to close decades [3-11]. Four dielectric relaxations modes were observed and ascribed to the mobility of different groups or to reorientation of cellulose-water complexes, but some points remain unraveled leading to multiple interpretations [12-14].

Dielectric properties of other types of fibers like polyester (PES) ones or of different mixtures were also studied motivated by the dependence of the relaxation processes on the motion of individual molecules and implicitly on the inter/intra-molecular interactions within the closest surroundings. Polyester fibers are poor conductors of direct current and a resistivity of the order of 10^{11} Ω .m; they have very good dielectric properties [15]. Investigations concerning their dielectric properties were performed for bulk or fabric material [16-28] In the dielectric loss spectrum of PES, two distinct relaxation processes were observed and attributed to the glass transition, associated with motions of main chain segments (α -relaxation), and a faster process related to the local motion of the C=O polar side groups (β -relaxation).

In this work we present the dielectric investigations on some composites containing polyester fabrics coated with ZnO by electroless deposition [29]. The characterization performed for the modified samples shows that though the surface of polyester is rather inactive, it was however changed by deposition. We made the dielectric measurements in a parallel capacitor between 10^{-2} and 10^7 Hz in a temperature interval from ca. 123 to 473 K, without taking into

* Corresponding author: lfrunza@infim.ro

consideration the inter-fiber air/nitrogen or the mesh size of the plane weave. (α - and β -relaxations of PES material were observed for the ZnO/PES composites as well. Additional modes, at intermediate frequency, was also observed in the composite case. The conductivity of the examined systems was further analyzed and discussed, although it is not yet completely understood. The temperature dependences of the characteristic frequencies and of the dielectric strength have only the expected Arrhenius form. Thus the study of dielectric constant and dielectric loss as a function of temperature and frequency has indicated a particular deposition of the ZnO particles at the microenvironment level.

2. Experimental

2.1 Samples

The investigated fabrics are made from polyester fibers. The raw (or original in the following) samples have the same composition but differ by the surface roughness: they have different yarn densities and “pores”/meshes; some of them are knitted fabric while others are in the woven fabric form. The plain samples with thickness ca. 0.5 mm, made up of 9-10 μm fibers are shortly described in Table 1.

Table 1 Properties of the investigated textile samples

| Sample label | Fiber nature | Textile 2D-element/thread | Color | Thickness /mm |
|--------------|--------------|----------------------------------|-------|---------------|
| PES3 | polyester | knitted fabric interlock/Nm 50/1 | white | 0.880 |
| PES5 | polyester | knitted fabric glat/Nm 50/1 | white | 0.519 |
| PES30 | polyester | woven fabric/Nm 70/2 + Nm 40/2 | white | 0.560 |

Before functionalization the plain weave was cut at the dimensions of $\sim 20 \times 20$ mm and carefully cleaned [29]. Textile surface was modified by deposition of zinc oxide nanoparticles using the electroless method by a treatment in three steps as follows: i) Sensitization in a solution containing tin(II) ions; ii) Activation in a solution containing palladium(II) ions; iii) ZnO deposition from aqueous zinc nitrate–dimethylamine borane solution [29]. Finally the deposited samples were carefully rinsed with distilled water and dried under the ambient atmosphere.

2.2 Investigation methods

Routine sample characterization considered both the original and the deposited fabrics as well such as the structure, the surface morphology and the deposition changes. *X-ray diffraction* (XRD) made with a D8 Advance (Bruker-AXS) equipment with a CuK_α radiation (K_β radiation was eliminated) allowed phase identification; the qualitative aspects were obtained by Rietveld refining the data. *Scanning Electron Microscope* (SEM) images were taken with a Zeiss Evo 50 XVP instrument after conventional metallization of the samples by means of a plasma sputtering apparatus. *Thermo gravimetric* (TG) analysis [30] was performed in order to estimate the amount of ZnO deposited upon the fabrics; a Diamond TG-DTA apparatus (Perkin Elmer) in a temperature range of 30-800 $^\circ\text{C}$, at a heating rate of 10 K/min, working with dried air flow was used.

We have applied *broadband dielectric spectroscopy* (BDS) in the aim to observe the modifications brought by the ZnO particles to the dielectric permittivity values.

The equipment to measure the complex dielectric function $\varepsilon^*(f) = \varepsilon'(f) - i\varepsilon''(f)$ (f , frequency; ε' , real part; ε'' , loss part of the permittivity), was a high resolution ALPHA analyzer (Novocontrol, Germany) with an active sample head as presented in detail by Kremer and Schönhal's [31]. Samples were prepared in parallel plate geometry between two gold-plated electrodes of 10 mm diameter. Isothermal frequency scans were carried out. The temperature was

decreased/increased in steps of 2-5 K with temperature stability better than 0.1 K controlled by a Novocontrol Quatro cryosystem operating with dry nitrogen gas stream.

To analyze the data quantitatively and to separate the different relaxation processes, the model function of Havriliak-Negami [Error! Bookmark not defined.b] (HN) is employed

$$\varepsilon^*(f) - \varepsilon_\infty = \frac{\Delta\varepsilon}{(1 + (if/f_0)^\beta)^\gamma}$$

where f_0 is a characteristic frequency related to the frequency of maximal loss f_p (relaxation rate) of the relaxation process under consideration and ε_∞ describes the value of the real part ε' for $f \gg f_0$. β and γ are fractional parameters ($0 < \beta \leq 1$ and $0 < \gamma \leq 1$) characterizing the shape of the relaxation spectra. $\Delta\varepsilon$ denotes the dielectric strength, which is proportional to the mean squared effective dipole moment and to the number of the fluctuating dipoles per unit volume. If more than one relaxation process was observed in the experimental frequency window, a sum of HN functions is fitted to the data (using Novocontrol Winfit program). To reduce the number of fit parameters, $\gamma = 1$ was assumed. Conduction effects were treated in the usual way by adding a conductivity contribution, $\sigma_0/\varepsilon_0(2\pi f)^x$, to the dielectric loss. σ_0 is a fitting parameter related to the dc conductivity of the sample, and ε_0 is vacuum dielectric permittivity. The parameter x ($0 < x \leq 1$) describes for $x < 1$ non-Ohmic effects in the conductivity (for details, see also ref [31d]). Fig. 1 gives a representative example of the fit with three HN-functions to the data. The conductivity is also introduced and the parameter related to the dc conductivity has reliable values of $10^{-12} - 10^{-11}$ S/cm.

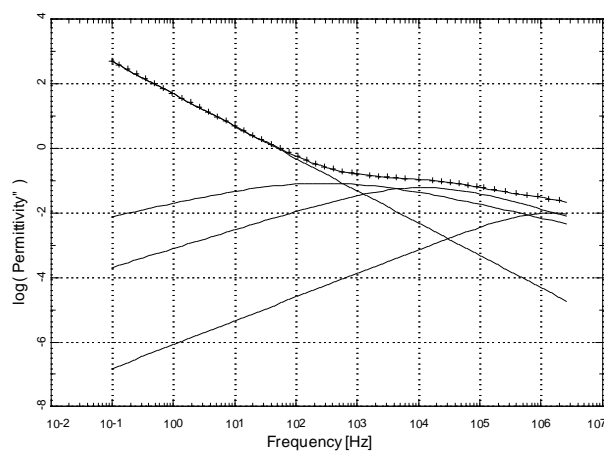


Fig. 1. Dielectric loss vs. frequency for the sample ZnO/PES30. The fitted HN functions are represented by solid lines, while the line through the experimental points is their sum.

3. Results and discussion

3.1 Sample characterization

Polyesters are sensitive to the manufacturing procedure, to the applied heat treatment, and to the conditions during service life, their response being related to the influence of external stimuli and environmental conditions. These polymers exhibit electrical relaxations phenomena, associated with glass transition, segmental mobility of polar groups, interfacial phenomena, and crystallization processes.

For our polymer composites in the solid state, the dielectric behavior is determined to a great extent by the physical structure; that is why the properties of the polyester fabric deposited with ZnO particles were carefully investigated in comparison with those of the original samples.

The morphologies of ZnO particles grown on the investigated fabrics were characterized by SEM. Representative micrographs are given in Fig. 2 for a raw sample and ZnO functionalized one.

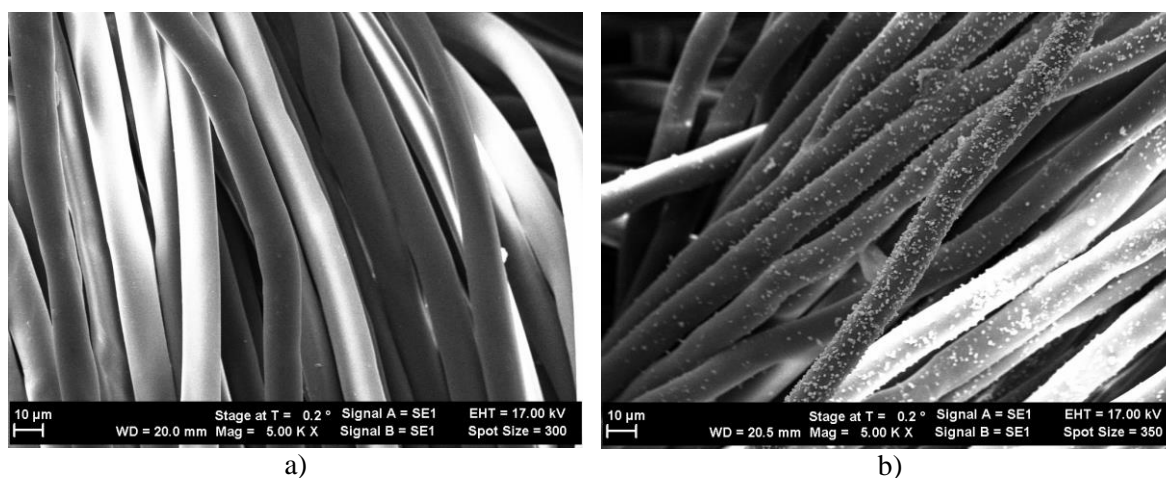


Fig. 2. SEM images (at the same magnification of 5000) of the PES5 sample a) in the original form; b) deposited with ZnO particles.

The images show that the ZnO crystallites have grown at the fibers surfaces. Apparently, each individual fiber looks like uniformly covered with densely packed micro- and nano-particles of hexagonal prism or bipod type having the basic size ranging from 20 to 500 nm, and a length scale of 0.7–1 μm . ZnO particles with hexagonal top-end suggest a *c*-axis growth of ZnO, which is confirmed by the corresponding XRD results. The particles show mostly a radial orientation, but some parallel growths might be also observed.

XRD studies were performed in the aim to observe the phases and the crystallinity of the investigated samples. Representative diffractograms of the original and deposited textile materials are given in Fig. 3. The raw materials present some large and wide reflections at low-to-medium 2θ angles due to their (semi)crystalline nature. The peaks can be assigned according to the literature. PES fibers give three broad peaks between 15° and 30° in an intensity sequence similar to that found in Ref. [32], peaks which are due to the reflections on the planes (010), (110) and (100) respectively [33]. A crystallinity index from the fixed count measurements at 26° and 28.6° [Error! Bookmark not defined.] cannot be evaluated because our PES samples still have too high intensity at 28.6° which disturbs this evaluation.

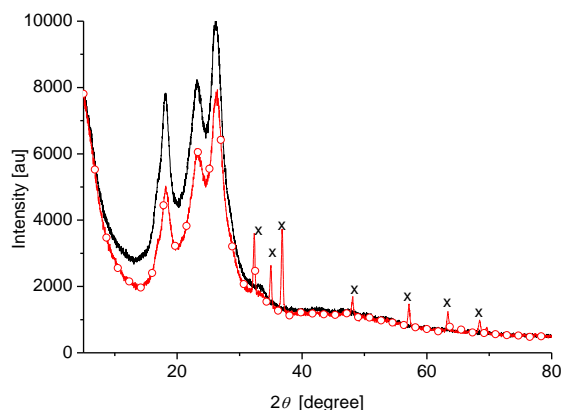


Fig. 3. XRD pattern of the original PES30 (line) and the corresponding ZnO deposited sample (line + empty circles). The positions of the peaks due to hexagonal ZnO phase are "x" marked.

ZnO deposited samples have XRD patterns (Fig. 3) with the polymer peaks similar to the corresponding raw materials; the additional sharp reflections appeared in these patterns can be indexed to the pure hexagonal wurtzite phase of ZnO (space group: $P63mc$) with lattice constants a and c which are in good agreement with the ICSD parameters of $a = 3.2498 \text{ \AA}$ and $c = 5.2066 \text{ \AA}$. These sharp peaks appear at $2\theta = 32.01^\circ$, 34.65° and 36.42° and correspond to the reflections (100), (001) and (101) respectively; ZnO crystal grows mostly along (001) [34]. The mean crystallite size (given by Rietveld refinement) is ca. 60 nm, in good agreement with the SEM results, though SEM “sees” particular particles. From Fig. 4, a decrease of the intensity of PES crystalline peaks when adding (nano)oxide can also be observed. This intensity decrease could be due to the higher absorption of nanoparticles that have higher density (5.6 g.cm^{-3}) than the polymer, and partially, to the decrease of crystallinity [35] by the effect of ZnO (nano)particles in hindering the motion of the polymer chain segments in the fibers by analogy with the explanation found by Panaitescu *et al.* in the case of inorganic oxide fillers of polyethylene[35].

Thermo gravimetric (TG) analysis is based on the presence of inorganic oxide over ca. 900 K, while the organic fiber part was burned off at much lower temperatures; then, one can estimate the amount of the ZnO on the fabric samples which is ca. 7.5(-10) %. Figure 4 presents TG and DTG curves for the PES3 and ZnO/PES3 materials which are representative for the investigated samples.

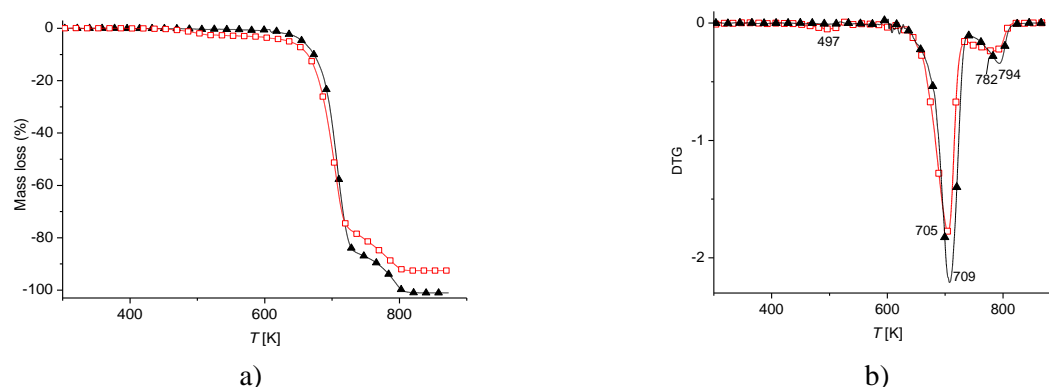


Fig. 4. Curves of thermal analysis for PES3 (filled symbols) and ZnO/PES3 (empty symbols) samples: a) TG curves; b) corresponding DTG curves.

Thermal events are expected at 348K, 423K and 525K due to glass/rubber transition, cold crystallization exotherm, and melting endotherm respectively [36]. However, the weight must be unchanged during these events and this can be indeed seen in Fig. 4.

The infrared spectroscopic studies should lead to information about the characteristic groups in the material fibers and to their relation with the deposited ZnO particles. However, we observed (the spectra were not shown here) that the main vibrations are less affected by the deposition of ZnO particles ZnO deposited cellulose [37]., meaning that the groups responsible for these vibrations are not directly reacting with the modifying particles unless partly, mostly in the region of OH stretching vibrations as in the related case of

3.2 Dielectric properties

BDS has been for a long time proven to be a powerful tool for the investigation of molecular mobility, phase changes, conductivity mechanisms, interfacial effects in polymers and their complex systems (see general reviews [Error! Bookmark not defined.a] or works devoted to specific topics [35, 38-40] Pioneer work concerning the dielectric properties of PES materials, carried out by Reddish, Mueller, Saito, Yamafuji, Mikhailov, Ishida, is summarized in refs. [31,41].

Though the real and the loss part of the dielectric function are interconnected each other by the Kramers-Kronig relationships, we present shortly the real dielectric constant and then the dielectric loss in order to facilitate the comparison with the literature data. Their frequency and/or their temperature dependence were obtained and considered for analysis.

Fig. 5 presents the real part of the apparent dielectric permittivity (dielectric constant) obtained for a representative sample. ϵ_a' increases (a little) with increasing the temperature. The variation with temperature of ϵ_a' is known to depend on the polymer polarity (or type). For example in the case of strong polar polymers the dielectric permittivity has to increase with increasing temperature [42], as also found in the case of polyester textiles [**Error! Bookmark not defined.**]. This increase might be attributed to greater freedom of the molecular chain movement at high temperature [**Error! Bookmark not defined.**], which leads to increased polarization.

ϵ_a' values for ZnO/PES3 (see Fig. 5) and ZnO/PES5 samples are higher than for the original fibers, probably due to a major contribution of the interfacial polarization, determined by the increased number of charges (impurities and small ions) introduced in the polymer by the nanoparticles. This behavior could also be explained by the nanofiller dispersion [**Error! Bookmark not defined.**]. Other authors found the decrease of the dielectric constant with increasing temperatures for polyethylene filled with ZnO whiskers [43]. In the case of ZnO/PES30 (not shown here), the presence of the nanoparticles leads to a decreased permittivity with respect to the original PES samples: the deposited sample behaves as having a reduced movement of the chain due to the presence of these ZnO particles. In fact, the behavior of our latter case discussed was in agreement with the dielectric constant of the silica/polymer composite reduced to a lower value than that of original epoxy polymer [44] by containing a large amount of low dielectric air (with dielectric constant ~ 1).

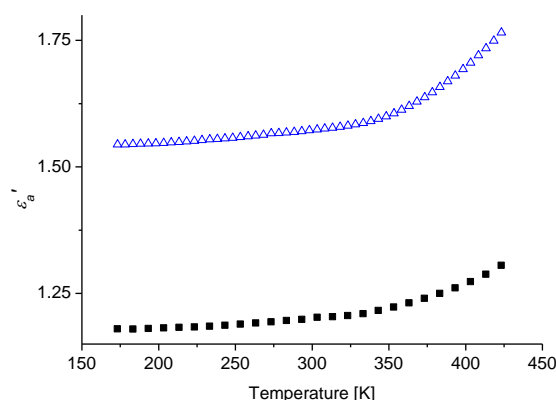


Fig. 5. Temperature dependence of the real part of the apparent dielectric permittivity at the frequency of ca. 1 MHz, for the samples PES3 (filled symbols) and ZnO/PES3 (empty symbols).

The imaginary part (dielectric loss) of the apparent dielectric permittivity is given in a 3D representation in Fig. 6 for the samples in the original and deposited form, during cooling. There is a complex dependence of the dielectric loss on the frequency and temperature, first an increase with increasing temperature up to a peak maximum followed by a reversion with further temperature rise.

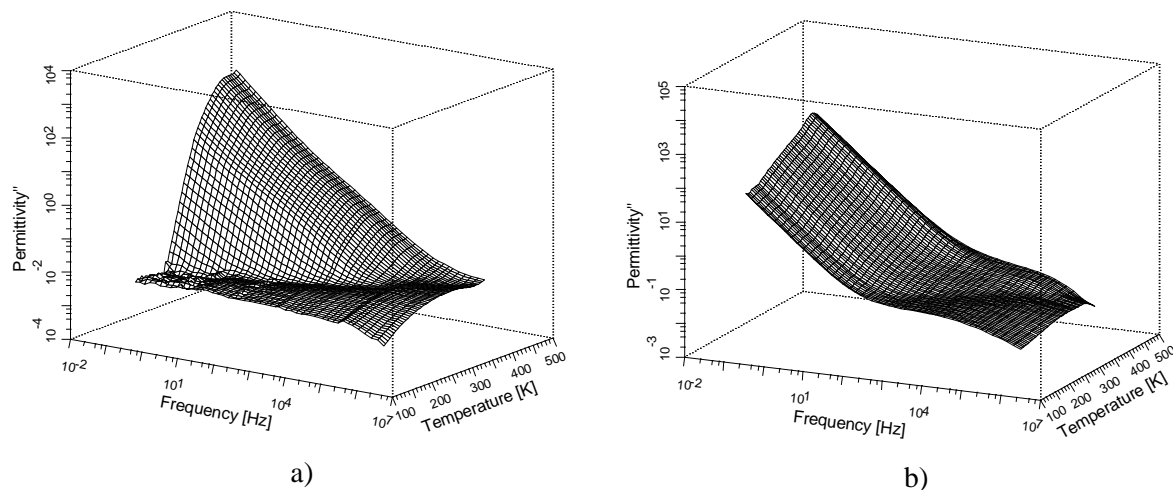


Fig. 6. Apparent dielectric loss versus frequency and temperature measured during cooling for the samples: a) PES3; b) ZnO/PES3.

The peak maximum of dielectric loss shows slight shift towards higher temperature which might be explained [Error! Bookmark not defined.] as being due to compatibility and enhancement of ZnO modifying particles (the effect of interface between the PES matrix and ZnO fillers). The maximum position of ε_a'' shifts with temperature changes: higher the temperature higher the frequency of the maximum due to the increased local segmental motion of polymeric materials. At the same time, there is a very small increase of the height of the maximum for all measured samples, due to the low polarity of the PES molecules, since the polar ester groups have the dipole moment equal to 0.7 D [45]. In the original samples, the maximum of relaxation is at frequency of ca. 10^5 Hz and at 300 K, as found in the literature [Error! Bookmark not defined., Error! Bookmark not defined.]. The loss peak is rather weak, broad and symmetrical, which is associated with a good degree of crystallinity. In addition, several relaxation processes can be then inferred. Thus, the textile materials have a semi-crystalline (crystalline and amorphous regions) fiber structure [Error! Bookmark not defined.]. Their ε'' can show different dielectric relaxations designated as α , β , γ or δ . One can say that the α -relaxation is associated with motions of chain units of the crystalline part of the polymer. The β -relaxation process results from the motion of side branches, as well as of the chain-end motion. The γ -relaxation is associated with the dynamics of single monomer units. These three relaxations have been extensively studied. Due to the fact that these relaxations appear in different parts of the polymer, dielectric relaxation investigation enables detecting the structure change in those regions. Other works [Error! Bookmark not defined.] assigns the relaxation processes observed in the polyester (and its copolymer) materials in this low frequency domain (at 383 K) to interfacial relaxation (α^*) and to the dipole relaxation (α) while Merenga et al. [Error! Bookmark not defined.] speak about a β^* relaxation as being a weak process on the low frequency side of the broad and strong process (due to β relaxation). The origin of the β -relaxation in PES has been attributed to the motion of the phenyl rings below the glass transition temperature [46,47]. Moreover, it is shown that the high temperature side of the relaxation peak is due to phenyl ring flips, whereas the low temperature side is due to the motion of the carbonyl groups; besides, it appeared that the activation energy and the enthalpy of the phenyl ring flips are both considerably higher than that of the carbonyls [46]. Hence, the assignment of the relaxation processes in the polymer materials does not receive yet the total agreement. One more point of view is that β -relaxation comes from localized rotational fluctuation of the electric dipoles while α relaxation is associated with the dynamic glass transition or to the overall chain dynamics [Error! Bookmark not defined.f].

The mean relaxation rate f_p (frequency of maximum dielectric loss) or the derived relaxation time $\tau=1/(2\pi f_p)$ (further we have dropped the “a” apparent sign in the name of relaxation rate or time) and the values of dielectric strength $\Delta\varepsilon$ were obtained in temperature dependence for each relaxation process. Figure 7 gives representative temperature dependencies as function of the inverse temperature. The dependence obeys either the Arrhenius law:

$$f_p = f_\infty \exp[-E_A/k_B T] \quad (2)$$

with E_A , activation energy; f_∞ , pre-exponential factor; k_B , Boltzmann’ s constant; T , temperature. The parameters resulted in our fits (as mentioned in Table 2) have reliable values [48,49]. Activation energy, with relatively low values estimated of ca. 26-30 kJ/mol and the prefactor $\log(f_\infty$ [Hz]) with values of 10-12 point to quite localized molecular fluctuations. A detailed assignment would require additional investigation. Higher activation energy values are around 50 kJ/mol and the corresponding prefactors are 10-12: The Arrhenius behavior is obvious. In other cases, the behavior is less obvious.

Table 2 Parameters of the Arrhenius dependence of the dielectric spectra

| Sample | E_a | f_∞ | Sample | E_a | f_∞ |
|--------|-------------|------------|-----------|-----------|------------|
| PES3 | 30.0 (lf*) | 5.62 | ZnO/PES3 | 14.5 (lf) | 4.71 |
| | 43.0 (hf**) | 12.8 | | 12.0 (hf) | 6.6 |
| PES5 | 62.8 (lf) | 10.6 | ZnO/PES5 | 56.8 | 14.5 |
| | 26.7 (hf) | 10.6 | | | |
| PES30 | 3.7 (lf) | 1.1 | ZnO/PES30 | 14.1 | 5.1 |
| | 2.3 (hf) | 0.9 | | | |

*lf = low frequency branch; **hf = high frequency branch

The Vogel–Fulcher–Tammann (VFT) law:

$$\log f_p = \log f_\infty - \frac{A}{T - T_0}$$

where A is a constant and T_0 is so-called Vogel or ideal glass temperature can be also looked for the temperature dependence of the relaxations, especially for the α -processes. However, due to the complexity of the materials and of the decomposition, we did not use this form to fit the data.

Representative temperature dependence of the relaxation rate f_p of main relaxation peaks for original PES3 and ZnO/PES3 samples is presented in Fig. 7. The dielectric strength appears also. The dielectric spectra were complex and consequently, the decomposition into components was difficult (see the Schlosser and Schönhals program allowing a better guide and control of the mathematical paths [50]).

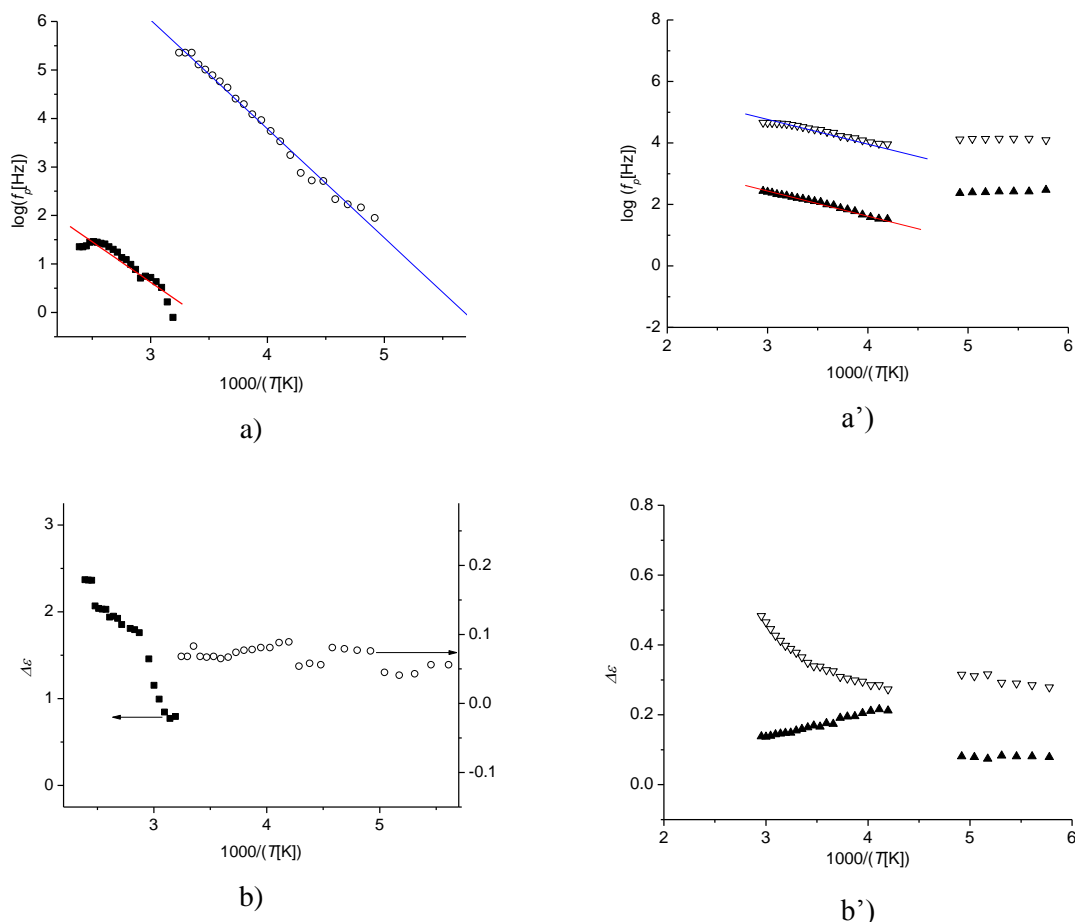


Fig. 7. Relaxation rates (a,a') and the corresponding values of dielectric strength (b,b') as function of the inverse temperature of the samples: a,b) PES3; a',b') ZnO/PES3. The solid lines represent the fit by Arrhenius law to the HN decomposition data.

In the original sample (Fig. 7a), a relaxation process can be seen at higher temperatures, having rather high dielectric strength. Instead of this, the other process seems to be observed at lower temperatures and has a low and almost constant dielectric strength. In the ZnO deposited sample, we may distinguish among the resulted relaxations, two different processes corresponding to the processes of the original sample. This might be interpreted as the influence of the deposited particles which is not uniform upon the fiber surface: thus, the obtained temperature variation might reflect the variety of the microscopic environment of the polymer chains.

Thus the study of the dielectric behavior offers a diagnostic tool since it might reflect the molecular structure, the (dipole) motions and their mutual influence inside the material.

4. Conclusions

The molecular mobility of polyester textiles either in original form or modified by deposition of ZnO particles was investigated by dielectric spectroscopy in a large frequency and temperature range, which allows a detailed investigation and characterization of the relaxation behavior taking place in these structures. These measurements were supplemented by SEM, XRD, TGA analysis, and FTIR investigations in the aim to detect structural changes, which might appear during the thermal treatments.

SEM micrographs have shown that each fiber is rather uniformly covered with densely packed micro- and nano-particles of hexagonal prism or bipod type.

XRD investigations indicated semi-crystalline polymer material and crystalline ZnO particles.

TGA data show to evaluate the amount of ZnO deposited in each case. The zinc oxide particles were in the percentage of 7.5 %.

FTIR spectra confirmed that the samples has the described composition and structure.

The dielectric permittivity was found to be decreased with increasing frequency and temperature as expected due to the polar nature of the polyester. Thus, the dielectric spectra of original polyester materials show at least two relaxation processes in the investigated temperature range and frequency windows: one process at lower temperatures and others at higher temperatures. A detailed analysis of the temperature dependence of the relaxation rates has shown that all these relaxation processes follow an Arrhenius dependence from which the activation energy for each is estimated.

ZnO particles induce changes in the morphology and electrical characteristics of polyester fibers. The changes in morphology consist in a small decrease of PES crystallinity.

The results of dielectric characterization emphasize different dielectric behaviors of the nano-composites, depending on the frequency and on the fabric structure. Smaller permittivity values than those of the base polymer were observed for one PES nano-composite sample.

The dielectric properties of the composites can be easily compared each other since the amount of ZnO particles is similar. Besides, the support materials have the same composition. The samples are differentiated by their roughness.

Acknowledgements

The authors thank the Romanian National Research Council for the financial support under the project ID281/2011. The logistic support of BAM Federal Institute of Materials Research and Testing (Berlin, Germany) and the permanent support from Professor Dr. Andreas Schönhals (BAM) are gratefully acknowledged.

References

- [1] J. Lesnikowski, *Przegląd Elektrotechniczny (Electrical Review)* **88**, 148 (2012).
- [2] K. Bal, V.K. Kothari, *Indian J. Fibre&Textile Res.* **34**, 191 (2009).
- [3] J. Einfeldt, D. Meissner, A. Kwasniewski, *Macromol. Chem. Phys.* **201**, 1969 (2000).
- [4] J. Einfeldt, D. Meissner, A. Kwasniewski, E. Gruber, R. Henricks, *Macromol. Mater. Engn.* **283**, 7 (2000).
- [5] D. Meissner, J. Einfeldt, A. Kwasniewski, *J. Non-Cryst. Solids* **275**, 199 (2000).
- [6] J. Einfeldt, D. Meissner, A. Kwasniewski, *Progr. Polymer Sci.* **26** 1419 (2001).
- [7] J. Einfeldt, D. Meissner, A. Kwasniewski, *J. Non-Cryst. Solids* **320**, 40 (2003).
- [8] J. Einfeldt, D. Meissner, A. Kwasniewski, *Cellulose* **11**, 137 (2004).
- [9] G. Jafarpour, E. Dantras, A. Boudet, C. Lacabanne, *J. Non-Cryst. Solids* **353**, 4108 (2007).
- [10] G. Jafarpour, F. Roig, E. Dantras, A. Boudet, C. Lacabanne, *J. Non-Cryst. Solids* **355**, 1669 (2009).
- [11] F. Roig, E. Dantras, J. Dandurand, C. Lacabanne, *J. Phys. D: Applied Physics*, **44**, 045403 (2011).
- [12] M. Kent, W. Meyer, *J. Phys. D: Appl. Phys.* **16**, 915–925 (1983).
- [13] H. Sugimoto, T. Miki, K. Kanayama, M. Norimoto, *J. Non-Cryst. Solids* **354**, 3220 (2008).
- [14] V. Svedas, *J. Phys. D: Appl. Phys.* **31**, 1752 (1998).
- [15] S. Hausman, Ł. Januszkiewicz, M. Michalak, T. Kacprzak, I. Krucińska, *Fibres & Textiles Eastern Eur.* **14**, 60 (2006).
- [16] W. Reddish, *Trans. Fraday Soc.* **46**, 459 (1950).
- [17] J.W.S. Hearle, *Text. Res. J.* **24**, 307 (1954).
- [18] J.W.S. Hearle, *Text. Res. J.* **26**, 108 (1956).
- [19] E.E. Smirnova, K.E. Perepelkin, N.A. Smirnova, S.A. Brezgina, *Fibre Chem.* **34**, 192 (2002).

- [20] D.D. Cerovic, J.R. Dojcilovic, K. A. Asanovic, T.A. Mihajlidi, *J. Appl. Phys.* **106**, 084101 (2009).
- [21] D.D. Cerovic, J.R. Dojcilovic, S.B. Maletic, *Eur. Polymer J.* **48**, 850 (2012).
- [22] I.M. Ward, A.S. Maxwell, L. Monnerie, *Polymer* **39**, 6835 (1998); idem, *Polymer* **39**, 6851 (1998).
- [23] A.S. Merenga, C. M. Papadakis, F. Kremer, J. Liu, A.F. Yee, *Colloid Polym. Sci.* **279**, 1064 (2001).
- [24] D.D. Cerovic, K.A. Asanovic, S.B. Maletic, J.R. Dojcilovic, *Composites: Part B* **49**, 65 (2013).
- [25] E. Carsalade, A. Bernès, C. Lacabanne, S. Perraud, M. Lafourcade, M. Savignac, *J. Thermal Anal. Calorim.* **101**, 849 (2010).
- [26] E. Neagu, P. Pissis, L. Apekis, and J. L. Gomez Ribelles, *J. Phys. D: Appl. Phys.* **30**, 1551 (1997); E. Neagu, P. Pissis, L. Apekis, *J. Appl. Phys.* **87**, 2914 (2000).
- [27] M. Akram, A. Javed, T. Z. Rizvi, *Turk. J. Phys.* **29**, 355 (2005).
- [28] D. Alperstein, M. Narkis, A. Siegmann, B. Binder, *Polymer Eng. Sci.* **35**, 284 (1995).
- [29] L. Frunza, N. Preda, E. Matei, S. Frunza, C. P. Ganea, A. M. Vlaicu, L. Diamandescu, A. Dorogan, *J. Polym. Sci. B: Polym. Phys.* **51**, 1237 (2013).
- [30] S. Frunza, H. Kosslick, A. Schonhals, L. Frunza, I. Enache, T. Beica, *J. Non-Cryst. Solids* **325**, 103 (2003).
- [31] F. Kremer, A. Schönhalz Eds., *Broadband Dielectric Spectroscopy*; Springer-Verlag: Berlin Heidelberg, 2003: (a) pp 35ff, (b) p 62, (c) p 22, (d) pp 133ff, (e) Chp. 1, (f) p 225.
- [32] V. Janickis, I. Ancutiene, J. Žukauskaite, *Mater. Sci.* **13**, 132 (2007).
- [33] N.V. Bhat, M.J. Kale, A.V. Gore, *J. Eng. Fibres Fabrics* **4**, 1 (2009).
- [34] J.H. Park, P. Muralidharan, D.K. Kim, *Mater. Lett.* **63**, 1019 (2009).
- [35] D. Panaitescu, F. Ciuprina, M. Iorga, A. Frone, C. Radovici, M. Ghiurea, S. Sever, I. Plesa, *J. Appl. Polym. Sci.* **122**, 1921 (2011).
- [36] G.C. Psarras, A. Soto Beobide, G.A. Oyiatis, P.K. Karahaliou, S.N. Georga, C.A. Krontiras, J. Sotiropoulos, *J. Polym. Sci. Part B: Polym. Phys.* **44**, 3078 (2006).
- [37] S.S. Ugur, M. Sarınsık, A.H. Aktas, M.C. Ucar, E. Erden, *Nanoscale Res. Lett.* **5**, 1204 (2010).
- [38] A.L. Alexe-Ionescu, G. Barbero, L. Komitov, *Phys. Rev. E* **80**, 021701 (2009).
- [39] I. Plesa, F. Ciuprina, P.V. Notingher, D. Panaitescu, *Rev. Roum. Sci. Techn. Electrotechn. et Energ.* **56**, 277 (2011).
- [40] T. Zaharescu, S. Jipa, E.D. Popescu, W. Kappel, G. Samoilescu, *Mater. Plastice* **45**, 285 (2008).
- [41] N.G. McCrum, B.E. Read, G. Williams, in *Anelastic and Dielectric Effects in Polymeric Solids*; Wiley: New York, 1964; 502–520.
- [42] F.U.Z. Chowdhury, A.H. Bhuiyan, *Thin Solid Films* **370**, 78 (2000).
- [43] Z. Dang, L. Fan, Y. Shen, C. Nan, S. Zhao, *J. Thermal Anal. Calorim.* **71**, 635 (2003).
- [44] N. Suzuki, S. Kiba, Y. Yamauchi, *Micropor. Mesopor. Mat.* **138**, 123 (2011).
- [45] K.E. Perepelkin, *Fibre Chem.* **33**, 340 (2001).
- [46] A.S. Maxwell, L. Monnerie, I.M. Ward, *Polymer* **39**, 6851 (1998).
- [47] J. Menegotto, P. Demont, A. Bernes, C. Lacabanne, *J. Polym. Sci. B: Polym. Phys.* **37**, 3494 (1999).
- [48] A. Nogales, A. Sanz, T. A. Ezquerra, *J. Non-Cryst. Solids* **352**, 4649 (2006).
- [49] A. Sanz, A. Nogales, N. Lotti, A. Munari, T.A. Ezquerra, *J. Non-Cryst. Solids* **353**, 3989 (2007).
- [50] E. Schlosser, A. Schonhals, *Colloid Polym. Sci.* **267**, 963 (1989).